Chapter 20

Cycle expansions

Recycle... It's the Law!
—Poster, New York City Department of Sanitation

The Euler product representations of spectral determinants (19.9) and dynamical zeta functions (19.15) are really only a shorthand notation - the zeros of the individual factors are *not* the zeros of the zeta function, and the convergence of these objects is far from obvious. Now we shall give meaning to dynamical zeta functions and spectral determinants by expanding them as *cycle expansions*, which are series representations ordered by increasing topological cycle length, with products in (19.9), (19.15) expanded as sums over *pseudo-cycles*, products of weights t_p of contributing cycles. The zeros of correctly truncated cycle expansions yield the desired leading eigenvalues of evolution operators, and the expectation values of observables are given by the cycle averaging formulas obtained from the partial derivatives of dynamical zeta functions (or spectral determinants).

For reasons of pedagogy in what follows everything is first explained in terms of dynamical zeta functions: they aid us in developing 'shadowing' intuition about the geometrical meaning of cycle expansions. For actual calculations, we recommend the spectral determinant cycle expansions of sects. 20.2.2 and 20.4.2. While the shadowing is less transparent, and the weights calculation is an iterative numerical algorithm, these expansions use full analytic information about the flow, and can have better convergence properties than the dynamical zeta functions. For example, as we shall show in chapter 23, even when a spectral determinant (19.6) is entire and calculations are super-exponentially convergent, cycle expansion of the corresponding dynamical zeta function (19.25) has a finite radius of convergence and captures only the leading eigenvalue, at exponentially convergent rate.

20.1 Pseudocycles and shadowing

How are periodic orbit formulas such as (19.15) evaluated? We start by computing the lengths and Floquet multipliers of the shortest cycles. This always requires numerical work, such as searches for periodic solutions via Newton's method; we shall assume for the purpose of this discussion that the numerics is under control, and that *all* short cycles up to a given (topological) length have been found. Examples of the data required for application of periodic orbit formulas are the lists of cycles given in exercise 13.14 and table 29.3. Sadly, it is not enough to set a computer to blindly troll for invariant solutions, and blithely feed those into the formulas that will be given here. The reason that this chapter is numbered 20 and not 6, is that understanding the geometry of the non–wandering set is a prerequisite to good estimation of dynamical averages: one has to identify cycles that belong to a given ergodic component (whose symbolic dynamics and shadowing is organized by its transition graph), and discard the isolated cycles and equilibria that do not take part in the asymptotic dynamics. It is important not to miss any short cycles, as the calculation is as accurate as the shortest cycle dropped - including cycles longer than the shortest omitted does not improve the accuracy (more precisely, the calculation improves, but so little as not to be worth while).

chapter 13

Given a set of periodic orbits, we can compute their weights t_p and expand the dynamical zeta function (19.15) as a formal power series,

$$1/\zeta = \prod_p (1 - t_p) = 1 - \sum_{\{p_1 p_2 \cdots p_k\}}{}' (-1)^{k+1} t_{p_1} t_{p_2} \cdots t_{p_k} \tag{20.1}$$

where the prime on the sum indicates that the sum is over all distinct non-repeating combinations of prime cycles. As we shall frequently use such sums, let us denote by $t_\pi = (-1)^{k+1} t_{p_1} t_{p_2} \cdots t_{p_k}$ an element of the set of all distinct products of the prime cycle weights t_p. The formal power series (20.1) is now compactly written as

$$1/\zeta = 1 - \sum_\pi{}' t_\pi \,. \tag{20.2}$$

For $k > 1$, the signed products t_π are weights of *pseudo-cycles*; they are sequences of shorter cycles that shadow a cycle with the symbol sequence $p_1 p_2 \ldots p_k$ along the segments p_1, $p_2, \ldots$, p_k, as in figure 1.12. The symbol $\sum'$ denotes the restricted sum, for which any given prime cycle p contributes at most once to a given pseudo-cycle weight t_π.

The pseudo-cycle weight, i.e., the product of weights (19.10) of prime cycles comprising the pseudo-cycle,

$$t_\pi = (-1)^{k+1} \frac{}{|\Lambda_\pi|} e^{\beta A_\pi - s T_\pi} z^{n_\pi} \,, \tag{20.3}$$

depends on the pseudo-cycle integrated observable A_π, the period T_π, the stability Λ_π, remark 5.1

$$\begin{aligned} \Lambda_\pi &= \Lambda_{p_1}\Lambda_{p_2}\cdots\Lambda_{p_k}\,, \qquad T_\pi = T_{p_1}+\ldots+T_{p_k} \\ A_\pi &= A_{p_1}+\ldots+A_{p_k}\,, \qquad n_\pi = n_{p_1}+\ldots+n_{p_k}\,, \end{aligned} \tag{20.4}$$

and, when available, the topological length n_π.

20.1.1 Curvature expansions

The simplest example is the pseudo-cycle sum for a system described by a complete binary symbolic dynamics. In this case the Euler product (19.15) is given by

$$\begin{aligned} 1/\zeta &= (1-t_0)(1-t_1)(1-t_{01})(1-t_{001})(1-t_{011}) \\ &\quad\times(1-t_{0001})(1-t_{0011})(1-t_{0111})(1-t_{00001})(1-t_{00011}) \\ &\quad\times(1-t_{00101})(1-t_{00111})(1-t_{01011})(1-t_{01111})\ldots \end{aligned} \tag{20.5}$$

(see table 15.1), and the first few terms of the expansion (20.2) ordered by increasing total pseudo-cycle length are:

$$\begin{aligned} 1/\zeta &= 1-t_0-t_1-t_{01}-t_{001}-t_{011}-t_{0001}-t_{0011}-t_{0111}-\ldots \\ &\quad +t_0t_1+t_0t_{01}+t_{01}t_1+t_0t_{001}+t_0t_{011}+t_{001}t_1+t_{011}t_1 \\ &\quad -t_0t_{01}t_1-\ldots \end{aligned} \tag{20.6}$$

We refer to such series representation of a dynamical zeta function or a spectral determinant, expanded as a sum over pseudo-cycles, and ordered by increasing cycle length and instability, as a *cycle expansion*.

The next step is the key step: regroup the terms into the dominant *fundamental* contributions t_f and the decreasing *curvature* corrections $\hat{c}_n$, each $\hat{c}_n$ split into prime cycles p of length $n_p{=}n$ grouped together with pseudo-cycles whose full itineraries build up the itinerary of p. For the binary case this regrouping is given by

$$\begin{aligned} 1/\zeta &= 1-t_0-t_1-[(t_{01}-t_1t_0)]-[(t_{001}-t_{01}t_0)+(t_{011}-t_{01}t_1)] \\ &\quad -[(t_{0001}-t_0t_{001})+(t_{0111}-t_{011}t_1) \\ &\quad\quad +(t_{0011}-t_{001}t_1-t_0t_{011}+t_0t_{01}t_1)]-\ldots \\ &= 1-\sum_f t_f-\sum_n \hat{c}_n\ . \end{aligned} \tag{20.7}$$

All terms in this expansion up to length $n_p = 6$ are given in table 20.1. We refer to such regrouped series as *curvature expansions*, because the shadowed combinations $[\cdots]$ vanish identically for piecewise-linear maps with nice partitions, such as the 'full tent map' of figure 16.3.

This separation into 'fundamental' and 'curvature' parts of cycle expansions is possible *only* for dynamical systems whose symbolic dynamics has finite grammar. The fundamental cycles t_0, t_1 have no shorter approximations; they are the "building blocks" of the dynamics in the sense that all longer orbits can be approximately pieced together from them. The fundamental part of a cycle expansion is given by the sum of the products of all non-intersecting loops of the associated transition graph, discussed in chapter 14. The terms grouped in brackets $[\cdots]$ are the curvature corrections; the terms grouped in parentheses $(\cdots)$ are combinations of longer cycles and corresponding sequences of "shadowing" pseudo-cycles, as in figure 1.12. If all orbits are weighted equally ($t_p = z^{n_p}$), such combinations cancel exactly, and the dynamical zeta function reduces to the topological polynomial (15.27). If the flow is continuous and smooth, orbits of similar symbolic dynamics will traverse the same neighborhoods and will have similar weights, and the weights in such combinations will almost cancel. The utility of cycle expansions of dynamical zeta functions and spectral determinants, in contrast to naive averages over periodic orbits such as the trace formulas discussed in sect. 22.4, lies precisely in this organization into nearly canceling combinations: cycle expansions are dominated by short cycles, with longer cycles giving exponentially decaying corrections.

section 15.3
section 20.5

More often than not, good symbolic dynamics for a given flow is either not available, or its grammar is not finite, or the convergence of cycle expansions is affected by non-hyperbolic regions of state space. In those cases truncations such as the *stability cutoff* of sect. 20.6 and sect. 24.3.4 might be helpful. The idea is to truncate the cycle expansion by including only the pseudo-cycles such that $|\Lambda_{p_1} \cdots \Lambda_{p_k}| \leq \Lambda_{\max}$, with the cutoff $\Lambda_{\max}$ equal to or greater than the most unstable Λ_p in the data set.

In what follows, we shall introduce two cycle averaging formulas, one based on dynamical zeta functions and the other on spectral determinants. (Frequently used, but inferior 'level sums' shall be discussed in sect. 22.4.)

20.2 Construction of cycle expansions

Due to the lack of factorization of the determinant in the denominator of the full pseudo-cycle weight in (18.23),

$$\det\left(\mathbf{1} - M_{p_1 p_2}\right) \neq \det\left(\mathbf{1} - M_{p_1}\right) \det\left(\mathbf{1} - M_{p_2}\right) ,$$

the cycle expansions for the spectral determinant (19.9) are somewhat less transparent than is the case for the dynamical zeta functions, so we postpone their

Table 20.1: The binary curvature expansion (20.7) up to length 6, listed in such a way that the sum of terms along the pth horizontal line is the curvature $\hat{c}_p$ associated with a prime cycle p, or a combination of prime cycles such as the $t_{100101} + t_{100110}$ pair.

$- t_0$			
$- t_1$			
$- t_{10}$	$+ t_1 t_0$		
$- t_{100}$	$+ t_{10} t_0$		
$- t_{101}$	$+ t_{10} t_1$		
$- t_{1000}$	$+ t_{100} t_0$		
$- t_{1001}$	$+ t_{100} t_1$	$+ t_{101} t_0$	$- t_1 t_{10} t_0$
$- t_{1011}$	$+ t_{101} t_1$		
$- t_{10000}$	$+ t_{1000} t_0$		
$- t_{10001}$	$+ t_{1001} t_0$	$+ t_{1000} t_1$	$- t_0 t_{100} t_1$
$- t_{10010}$	$+ t_{100} t_{10}$		
$- t_{10101}$	$+ t_{101} t_{10}$		
$- t_{10011}$	$+ t_{1011} t_0$	$+ t_{1001} t_1$	$- t_0 t_{101} t_1$
$- t_{10111}$	$+ t_{1011} t_1$		
$- t_{100000}$	$+ t_{10000} t_0$		
$- t_{100001}$	$+ t_{10001} t_0$	$+ t_{10000} t_1$	$- t_0 t_{1000} t_1$
$- t_{100010}$	$+ t_{10010} t_0$	$+ t_{1000} t_{10}$	$- t_0 t_{100} t_{10}$
$- t_{100011}$	$+ t_{10011} t_0$	$+ t_{10001} t_1$	$- t_0 t_{1001} t_1$
$- t_{100101}$	$- t_{100110}$	$+ t_{10010} t_1$	$+ t_{10110} t_0$
	$+ t_{10} t_{1001}$	$+ t_{100} t_{101}$	$- t_0 t_{10} t_{101}$ $- t_1 t_{10} t_{100}$
$- t_{101110}$	$+ t_{10110} t_1$	$+ t_{1011} t_{10}$	$- t_1 t_{101} t_{10}$
$- t_{100111}$	$+ t_{10011} t_1$	$+ t_{10111} t_0$	$- t_0 t_{1011} t_1$
$- t_{101111}$	$+ t_{10111} t_1$		

evaluation to sect. 20.2.2. Sect. 20.2.1 is a pedagogical warmup. In actual calculations, implementing the spectral determinant cycle expansions of sect. 20.2.2 is recommended. Correct objects are spectral determinants, and as using the correct object costs exactly the same as using the approximations, why settle for less?

20.2.1 Evaluation of dynamical zeta functions

Cycle expansions of dynamical zeta functions are evaluated numerically by first computing the weights $t_p = t_p(\beta, s)$ of all prime cycles p of topological length $n_p \leq N$, for given fixed β and s. Denote by the subscript (i) the ith prime cycle computed, ordered by the topological length $n_{(i)} \leq n_{(i+1)}$. The dynamical zeta function $1/\zeta_N$ truncated to $n_p \leq N$ cycles is computed recursively, by multiplying

$$1/\zeta_{(i)} = 1/\zeta_{(i-1)}[1 - t_{(i)} z^{n_{(i)}}] , \tag{20.8}$$

and truncating the expansion at each step to a finite polynomial in z^n, $n \leq N$. The result is the Nth order polynomial approximation

$$1/\zeta_N = 1 - \sum_{n=1}^{N} c_n z^n . \tag{20.9}$$

In other words, a cycle expansion is a Taylor expansion in the dummy variable z, where each term in the sum is raised to the topological cycle length. If both the number of cycles and their individual weights grow not faster than exponentially

with the cycle length, and we multiply the weight of each cycle p by a factor z^{n_p}, the cycle expansion converges for sufficiently small $|z|$. If the symbolic dynamics grammar is finite, the truncation cuttof N has to be larger than the length of longest cycle in the transition graph (15.15), for the salubrious effect of shadowing cancelations to kick in. If that is the case, further increases in N yield the exponentially decreasing corrections $\hat{c}_n$ in (20.7).

If the dynamics is given by an iterated mapping, the leading zero of (20.9) as a function of z yields the leading eigenvalue of the appropriate evolution operator. For continuous time flows, z is a dummy variable that we set to $z = 1$, and the leading eigenvalue of the evolution operator is given by the leading zero of $1/\zeta(s, \beta(s))$ as function of s.

20.2.2 Evaluation of traces and spectral determinants

We commence the cycle expansion evaluation of a spectral determinant by computing the trace formula (18.10) or (18.23). The weight of prime cycle p repeated r times is

$$t_p(z,\beta,r) = \frac{e^{r\beta\cdot A_p}\, z^{r\, n_p}}{\left|\det\left(\mathbf{1} - M_p^r\right)\right|} \qquad \text{(discrete time)} \tag{20.10}$$

$$t_p(s,\beta,r) = \frac{e^{r(\beta\cdot A_p - sT_p)}}{\left|\det\left(\mathbf{1} - M_p^r\right)\right|} \qquad \text{(continuous time)}\,. \tag{20.11}$$

For *discrete time*, the trace formula (18.10) truncated to all prime cycles p and their repeats r such that $n_p r \le N$,

$$\operatorname{tr}\frac{z\mathcal{L}}{1 - z\mathcal{L}}\Big|_N = \sum_{n=1}^{N} C_n z^n\,, \qquad C_n = \operatorname{tr}\mathcal{L}^n\,, \tag{20.12}$$

is computed as a polynomial in z by adding a cycle at the time:

$$\operatorname{tr}\frac{z\mathcal{L}}{1 - z\mathcal{L}}\Big|_{(i)} = \operatorname{tr}\frac{z\mathcal{L}}{1 - z\mathcal{L}}\Big|_{(i-1)} + n_{(i)} \sum_{r=1}^{n_{(i)}r\le N} t_{(i)}(z,\beta,r)\,.$$

For *continuous time*, we assume that the method of Poincaré sections assigns each cycle a topological length n_p. Than the trace formula (18.23) is also organized as a polynomial

$$\operatorname{tr}\frac{1}{s - \mathcal{A}}\Big|_N = \sum_{n=1}^{N} C_n z^n\,, \tag{20.13}$$

computed as:

$$\mathrm{tr}\,\frac{1}{s-\mathcal{A}}\Big|_{(i)} \;=\; \mathrm{tr}\,\frac{1}{s-\mathcal{A}}\Big|_{(i-1)} \;+\; T_{(i)}\sum_{r=1}^{n_{(i)}r\le N} t_{(i)}(s,\beta,r)\,z^{n_p r}$$

The periodic orbit data set (20.4) consists of the list of the cycle periods T_p, the cycle Floquet multipliers $\Lambda_{p,1},\Lambda_{p,2},\ldots,\Lambda_{p,d}$, and the cycle averages of the observable A_p for all prime cycles p such that $n_p \le N$. The coefficient of $z^{n_p r}$ is then evaluated numerically for the given parameter values (β, s). Always compute the leading eigenvalue of the evolution operator first, i.e., the escape rate $\gamma = -s_0$, in order to use it in calculation of averages of sect. 20.4 as a weight $e^{\gamma T_{(i)}}$ in (20.12). Now that we have an expansion for the trace formula (18.9) as a power series, we compute the Nth order approximation to the spectral determinant (19.3),

$$\det(1-z\mathcal{L})|_N = 1-\sum_{n=1}^{N} Q_n z^n\,, \quad Q_n = n\text{th cumulant}\,, \tag{20.14}$$

as follows. The logarithmic derivative relation (19.4) yields

$$\left(\mathrm{tr}\,\frac{z\mathcal{L}}{1-z\mathcal{L}}\right)\det(1-z\mathcal{L}) = -z\frac{d}{dz}\det(1-z\mathcal{L})$$

$$(C_1 z + C_2 z^2 + \cdots)(1 - Q_1 z - Q_2 z^2 - \cdots) = Q_1 z + 2Q_2 z^2 + 3Q_3 z^3 \cdots$$

so the nth order term of the spectral determinant cycle (or in this case, the cumulant) expansion is given recursively by the convolution trace formula expansion coefficients

$$Q_n = \frac{1}{n}\left(C_n - C_{n-1}Q_1 - \cdots C_1 Q_{n-1}\right)\,, \qquad Q_1 = C_1\,. \tag{20.15}$$

Given the trace formula (20.12) truncated to z^N, we now also have the spectral determinant truncated to z^N.

The same program can also be reused to compute the dynamical zeta function cycle expansion (20.9), by replacing $\prod\left(1-\Lambda_{(i),j}^{r}\right)$ in (20.12) by the product of expanding eigenvalues $\Lambda_{(i)} = \prod_e \Lambda_{(i),e}$. section 19.3

A few points concerning different cycle averaging formulas:

- The dynamical zeta functions is an approximation to spectral determinant that yields only the leading eigenvalue of the evolution operator. The cycle weights depend only on the product of expanding $|\Lambda_i|$ Floquet multipliers, so signs do no matter. For hyperbolic flows they converge exponentially with increasing cycle lengths.

Table 20.2: The 3-disk repeller escape rates computed from cycle expansions of the spectral determinant (19.6) and the dynamical zeta function (19.15), as functions of the maximal cycle length N. The disk-disk center separation to disk radius ratio is $R{:}a$, and the $\det(s-\mathcal{A})$ is an estimate of the classical escape rate computed from the spectral determinant cycle expansion in the fundamental domain. For larger disk-disk separations, the dynamics is more uniform, as illustrated by the faster convergence. Convergence of spectral determinant $\det(s-\mathcal{A})$ is super-exponential, see chapter 23. For comparison, the $1/\zeta(s)$ column lists estimates from the fundamental domain dynamical zeta function cycle expansion (20.7), and the $1/\zeta(s)_{\text{3-disk}}$ column lists estimates from the full 3-disk cycle expansion (20.35). The convergence of the fundamental domain dynamical zeta function is significantly slower than the convergence of the corresponding spectral determinant, and the full (unfactorized) 3-disk dynamical zeta function has still poorer convergence. (P.E. Rosenqvist.)

$R{:}a$	N	. $\det(s-\mathcal{A})$	$1/\zeta(s)$	$1/\zeta(s)_{\text{3-disk}}$
	1	0.39	0.407	
	2	0.4105	0.41028	0.435
	3	0.410338	0.410336	0.4049
6	4	0.4103384074	0.4103383	0.40945
	5	0.4103384077696	0.4103384	0.410367
	6	0.410338407769346482	0.4103383	0.410338
	7	0.410338407769346489		0.4103396
	8	0.4103384077693464893384		
	9	0.41033840776934648933846130		
	10	0.410338407769346489338461307819		
	1	0.41		
	2	0.72		
	3	0.675		
	4	0.67797		
3	5	0.677921		
	6	0.6779227		
	7	0.6779226894		
	8	0.6779226896002		
	9	0.677922689599532		
	10	0.67792268959953606		

- spectral determinants weights in (19.3) contain $1/|1-\Lambda_i|$ factors, so for them signs of Floquet multipliers Λ_i do matter. With finite grammar the leading eigenvalue converges super-exponentially in cycle length.

  Note that while the dynamical zeta functions weights use only the expanding Floquet multipliers $|\Lambda_e|$, for spectral determinants the weights are of form $|1-\Lambda_j^r|$, both expanding and contracting directions contribute, and the signs of multipliers do matter. That's why ChaosBook everywhere tracks multipliers Λ_j, rather than Floquet exponents λ_j. λ's belong to equilibria, periodic orbits require multipliers. That's the way cookie crumbles. For very high-dimensional flows (such as unstable periodic solutions of Navier-Stokes equations), usually only a subset of the most unstable / least contracting Floquet multipliers is known. As long as the contracting Floquet multipliers omitted from the weights in (20.12) are sufficiently strongly contracting, the errors introduced by replacement $|1-\Lambda_j^r| \to 1$ for such eigenvalues should be negligible.

- The least enlightened are the 'level sum' cycle averaging formulas. There is no point in using them, except that they have to be mentioned (here in sect. 22.4), as there is voluminous literature that uses them.

- Other formulas published in physics literature are likely to be wrong.

If the set of computed periodic orbits is incomplete, and their Floquet multipliers inaccurate, distinctions between different cycle averaging formulas are academic, as there are not sufficiently many cycles to start worrying about what expansion converges faster.

20.3 Periodic orbit averaging

The first cycle expansion calculation should always be the determination of the leading eigenvalue of the evolution operator, calculated as follows. After the prime cycles and the pseudo-cycles have been grouped into subsets of equal topological length, the dummy variable can be set equal to $z = 1$. With $z = 1$, the expansion (20.14) constitutes the cycle expansion (19.6) for the spectral determinant $\det(s-\mathcal{A})$. We vary s in cycle weights, and determine αth eigenvalue s_α (17.20) by finding $s = s_\alpha$ for which (20.14) vanishes. As an example, the convergence of a leading eigenvalue for a nice hyperbolic system is illustrated in table 20.2 by the list of pinball escape rates $\gamma = -s_0$ estimates computed from truncations of (20.7) and (20.14) to different maximal cycle lengths. chapter 23

The pleasant surprise, to be explained in chapter 23, is that one can prove that the coefficients in these cycle expansions decay exponentially or even faster, because of the analyticity of $\det(s-\mathcal{A})$ or $1/\zeta(s)$, for s values well beyond those for which the corresponding trace formula (18.23) diverges.

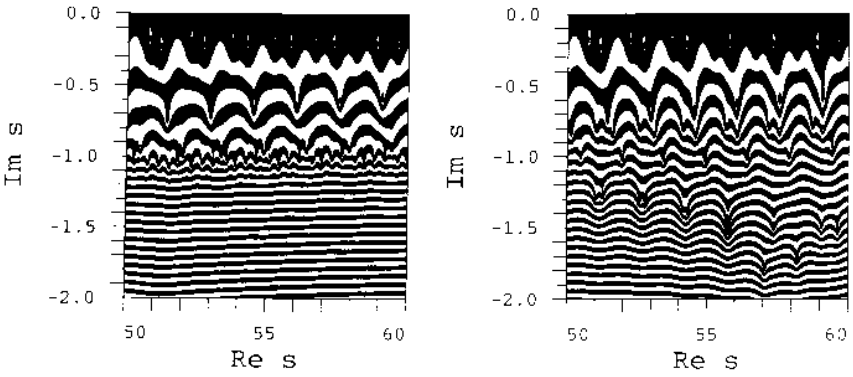

Figure 20.1: Example scans in the complex s plane: contour plots of the logarithm of the absolute values of (left) $1/\zeta(s)$, (right) spectral determinant $\det(s-\mathcal{A})$ for the 3-disk system, separation $R:a=6$. The A_1 subspace is evaluated numerically. The eigenvalues of the evolution operator $\mathcal{L}$ are given by the centers of elliptic neighborhoods of the rapidly narrowing rings. While the dynamical zeta function is analytic on the $\mathrm{Im}\, s \geq -1$ half-plane, the spectral determinant is entire and reveals further families of zeros. (P.E. Rosenqvist)

20.3.1 Newton algorithm for determining the evolution operator eigenvalues

Cycle expansions of spectral determinants can be used to compute a set of leading eigenvalues of the evolution operator. A convenient way to search for these is by plotting either the absolute magnitude $\ln|\det(s-\mathcal{A})|$ or the phase of spectral determinants and dynamical zeta functions as functions of the complex variable s. The eye is guided to the zeros of spectral determinants and dynamical zeta functions by means of complex s plane contour plots, with different intervals of the absolute value of the function under investigation assigned different colors; zeros emerge as centers of elliptic neighborhoods of rapidly changing colors. Detailed scans of the whole area of the complex s plane under investigation and searches for the zeros of spectral determinants, figure 20.1, reveal complicated patterns of resonances even for something as simple as the 3-disk game of pinball. With a good starting guess (such as the location of a zero suggested by the complex s scan of figure 20.1), a zero $1/\zeta(s)=0$ can now be determined by standard numerical methods, such as the iterative Newton algorithm (13.4), with the mth Newton estimate given by

$$s_{m+1} = s_m - \left(\zeta(s_m)\frac{\partial}{\partial s}\zeta^{-1}(s_m)\right)^{-1} = s_m - \frac{1/\zeta(s_m)}{\langle T\rangle_\zeta}\ . \tag{20.16}$$

The denominator $\langle T\rangle_\zeta$ is required for Newton iteration and is given by cycle expansion (20.25). We need to evaluate it anyhow, as $\langle T\rangle_\zeta$ is needed for the cycle averaging formulas.

Our next task will be to compute long-time averages of observables. Three situations arise, two of them equal in practice:

(i) The system is bounded, and we have all cycles up to some cutoff: always start by testing the cycle expansion sum rules of sect. 20.3.2.

(ii) The system is unbounded, and averages have to be computed over a repeller whose natural measure is obtained by balancing local instability with the global escape rate $\gamma = -s_0$, as in sect. 17.3.

(iii) The system is bounded, but we only have a repelling set consisting of a subset of unstable cycles embedded into the bounded strange attractor. Best one can do is to treat this as an open system, case (iii). That assigns a stationary natural measure to neighborhoods of the solutions used, the local instabilities balanced by a weight that includes escape rate $\exp(\gamma T_p)$. Whether use of this measure improves averages as one increases the stability cutoff depends on whether the longer cycles explore qualitatively different regions of state space not visited by the shorter (fundamental) cycles, or only revisit already known regions (curvature corrections).

20.3.2 Flow conservation sum rules

If a dynamical system is bounded, so that all trajectories remain confined for all times, the escape rate (22.8) vanishes $\gamma = -s_0 = 0$, and the leading eigenvalue of the Perron-Frobenius operator (16.10) (evolution operator with $\beta = 0$) is simply $\exp(-t\gamma) = 1$. Conservation of material flow thus implies that for bounded flows cycle expansions of dynamical zeta functions and spectral determinants satisfy exact *flow conservation* sum rules:

$$\begin{aligned} 1/\zeta(0,0) &= 1 + \sum_{\pi}{}' \frac{(-1)^k}{|\Lambda_{p_1}\cdots\Lambda_{p_k}|} = 0 \\ F(0,0) &= 1 - \sum_{n=1}^{\infty} Q_n(0,0) = 0 \end{aligned} \tag{20.17}$$

obtained by setting $s = 0$ in (20.18), (20.19) with cycle weights $t_p = e^{-sT_p}/|\Lambda_p| \to 1/|\Lambda_p|$. These sum rules depend neither on the cycle periods T_p nor on the observable $a(x)$ under investigation, but only on the cycle stabilities $\Lambda_{p,1}, \Lambda_{p,2}, \cdots, \Lambda_{p,d}$. Their significance is purely geometric; they are a measure of how well periodic orbits tessellate state space, as in figure 1.11. Conservation of material flow provides a first and very useful test of the quality of finite cycle length truncations and is something that you should always check when constructing a cycle expansion for a bounded flow.

20.4 Cycle formulas for dynamical averages

The eigenvalue conditions for the dynamical zeta function (20.2) and the spectral determinant (20.14),

$$0 = 1 - \sum_{\pi}{}' t_\pi\,, \qquad t_\pi = t_\pi(\beta, s(\beta)) \tag{20.18}$$

$$0 = 1 - \sum_{n=1}^{\infty} Q_n\,, \qquad Q_n = Q_n(\beta, s(\beta))\,, \tag{20.19}$$

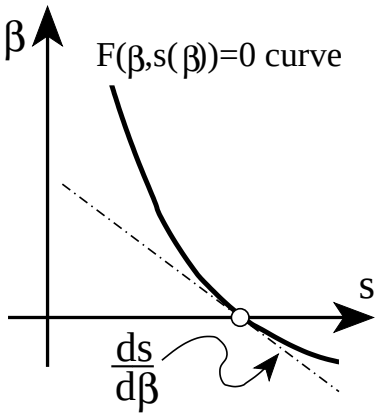

Figure 20.2: The eigenvalue condition is satisfied on the curve $F = 0$ on the (β, s) plane. The expectation value of the observable (17.12) is given by the slope of the curve.

are implicit equations for an eigenvalue $s = s(\beta)$ of the form $0 = F(\beta, s(\beta))$. The eigenvalue $s = s(\beta)$ as a function of β is sketched in figure 20.2; this condition is satisfied on the curve $F = 0$. The cycle averaging formulas for the slope and curvature of $s(\beta)$ are obtained as in (17.12) by taking derivatives of the eigenvalue condition. Evaluated along $F = 0$, by the chain rule the first derivative yields

$$\begin{aligned} 0 &= \frac{d}{d\beta}F(\beta, s(\beta)) \\ &= \frac{\partial F}{\partial \beta} + \frac{ds}{d\beta}\left.\frac{\partial F}{\partial s}\right|_{s=s(\beta)} \quad \Longrightarrow \quad \frac{ds}{d\beta} = -\frac{\partial F}{\partial \beta}\Big/\frac{\partial F}{\partial s}\,, \end{aligned} \tag{20.20}$$

and the second derivative of $F(\beta, s(\beta)) = 0$ yields

$$\frac{d^2 s}{d\beta^2} = -\left[\frac{\partial^2 F}{\partial \beta^2} + 2\frac{ds}{d\beta}\frac{\partial^2 F}{\partial \beta \partial s} + \left(\frac{ds}{d\beta}\right)^2 \frac{\partial^2 F}{\partial s^2}\right]\Big/\frac{\partial F}{\partial s}\,. \tag{20.21}$$

Denoting

$$\begin{aligned} \langle A\rangle_F &= -\left.\frac{\partial F}{\partial \beta}\right|_{\beta,s=s(\beta)}\,, \qquad \langle T\rangle_F = \left.\frac{\partial F}{\partial s}\right|_{\beta,s=s(\beta)}\,, \\ \left\langle (A-\langle A\rangle)^2\right\rangle_F &= \left.\frac{\partial^2 F}{\partial \beta^2}\right|_{\beta,s=s(\beta)}\,, \end{aligned} \tag{20.22}$$

respectively, and the mean cycle expectation value of A, the mean cycle period, and the second derivative of F computed for $F(\beta, s(\beta)) = 0$, we obtain the cycle averaging formulas for the expectation and variance of the observable (17.12):

$$\langle a\rangle = \frac{\langle A\rangle_F}{\langle T\rangle_F} \tag{20.23}$$

$$\left\langle (a-\langle a\rangle)^2\right\rangle = \frac{1}{\langle T\rangle_F}\left\langle (A-\langle A\rangle)^2\right\rangle_F\,. \tag{20.24}$$

These formulas are the central result of periodic orbit theory. We now show that for each choice of the function $F(\beta, s)$ in (20.2), (20.14), and (22.15), the above quantities have explicit cycle expansions.

20.4.1 Dynamical zeta function cycle averaging formulas

For the dynamical zeta function condition (20.18), the cycle averaging formulas (20.20), (20.24) require one to evaluate derivatives of dynamical zeta functions at a given eigenvalue. Substituting the cycle expansion (20.2) for the dynamical zeta function we obtain

$$\begin{aligned} \langle A\rangle_\zeta &:= -\frac{\partial}{\partial\beta}\frac{1}{\zeta} = \sum{}' A_\pi t_\pi \\ \langle T\rangle_\zeta &:= \frac{\partial}{\partial s}\frac{1}{\zeta} = \sum{}' T_\pi t_\pi\,, \quad \langle n\rangle_\zeta := -z\frac{\partial}{\partial z}\frac{1}{\zeta} = \sum{}' n_\pi t_\pi\,, \end{aligned} \tag{20.25}$$

where the subscript in $\langle\cdots\rangle_\zeta$ stands for the dynamical zeta function average over prime cycles, A_π, T_π, and n_π given by (20.3) are evaluated on pseudo-cycles (20.4), and pseudo-cycle weights $t_\pi = t_\pi(z,\beta,s(\beta))$ are evaluated at the eigenvalue $s(\beta)$. In most applications $\beta = 0$, and $s(\beta)$ of interest is typically the leading eigenvalue $s_0 = s_0(0)$ of the evolution generator $\mathcal{A}$.

For bounded flows the leading eigenvalue (the escape rate) vanishes, $s(0) = 0$, the exponent $\beta A_\pi - sT_\pi$ in (20.3) vanishes, so the cycle expansions take a simple form

$$\langle A\rangle_\zeta = \sum_\pi{}' (-1)^{k+1}\frac{A_{p_1}+A_{p_2}\cdots+A_{p_k}}{|\Lambda_{p_1}\cdots\Lambda_{p_k}|}\,, \tag{20.26}$$

where analogous formulas hold for $\langle T\rangle_\zeta$, $\langle n\rangle_\zeta$.

Example 20.1 ***Cycle expansion for the mean cycle period:*** *For example, for the complete binary symbolic dynamics the mean cycle period $\langle T\rangle_\zeta$ is given by* section 1.5.4

$$\begin{aligned} \langle T\rangle_\zeta &= \frac{T_0}{|\Lambda_0|}+\frac{T_1}{|\Lambda_1|}+\left(\frac{T_{01}}{|\Lambda_{01}|}-\frac{T_0+T_1}{|\Lambda_0\Lambda_1|}\right) \\ &\quad +\left(\frac{T_{001}}{|\Lambda_{001}|}-\frac{T_{01}+T_0}{|\Lambda_{01}\Lambda_0|}\right)+\left(\frac{T_{011}}{|\Lambda_{011}|}-\frac{T_{01}+T_1}{|\Lambda_{01}\Lambda_1|}\right)+\ldots\,. \end{aligned} \tag{20.27}$$

Note that the cycle expansions for averages are grouped into the same shadowing combinations as the dynamical zeta function cycle expansion (20.7), with nearby pseudo-cycles nearly canceling each other.

The cycle averaging formulas for the expectation of observable $\langle a\rangle$ follow by substitution into (20.24). Assuming zero mean drift $\langle a\rangle = 0$, the cycle expansion (20.14) for the variance $\left\langle (A-\langle A\rangle)^2\right\rangle_\zeta$ is given by

$$\left\langle A^2\right\rangle_\zeta = \sum{}' (-1)^{k+1}\frac{\left(A_{p_1}+A_{p_2}\cdots+A_{p_k}\right)^2}{|\Lambda_{p_1}\cdots\Lambda_{p_k}|}\,. \tag{20.28}$$

20.4.2 Spectral determinant cycle expansions

The dynamical zeta function cycle expansions have a particularly simple structure, with the shadowing apparent already by a term-by-term inspection of table 20.2. For "nice" hyperbolic systems, shadowing ensures exponential convergence of the dynamical zeta function cycle expansions. This, however, is not the best achievable convergence. As will be explained in chapter 23, for nice hyperbolic systems the spectral determinant constructed from the same cycle database is entire, and its cycle expansion converges faster than exponentially. The fastest convergence is attained by the spectral determinant cycle expansion (20.19) and its derivatives. In this case the $\partial/\partial s$, $\partial/\partial\beta$ derivatives are computed recursively, by taking derivatives of the spectral determinant cycle expansion contributions (20.12) and (20.15).

section 23.5

The cycle averaging formulas are exact, and highly convergent for nice hyperbolic dynamical systems. An example of their utility is the cycle expansion formula for the Lyapunov exponent of example 20.2. Further applications of cycle expansions will be discussed in chapter 22.

20.4.3 Continuous vs. discrete mean return time

Sometimes it is convenient to compute an expectation value along a flow in continuous time, and sometimes it might be easier to compute it in discrete time, from a Poincaré return map. Return times (3.1) might vary wildly, and it is not at all clear that the continuous and discrete time averages are related in any simple way. As we shall now show, the relationship turns out to be both elegantly simple, and totally general.

exercise 20.13

The mean cycle period $\langle T\rangle_\zeta$ fixes the normalization of the unit of time; it can be interpreted as the average near recurrence or the average first return time. For example, if we have evaluated a billiard expectation value $\langle a\rangle$ in terms of continuous time, and would like to also have the corresponding average $\langle a\rangle_{\rm dscr}$ measured in discrete time, given by the number of reflections off billiard walls, the two averages are related by

$$\langle a\rangle_{\rm dscr} = \langle a\rangle \langle T\rangle_\zeta / \langle n\rangle_\zeta \ , \tag{20.29}$$

where $\langle n\rangle_\zeta$ the average of the number of bounces n_p along the cycle p is given by is (20.25).

Example 20.2 ***Cycle expansion formula for Lyapunov exponents:*** *In sect. 17.4 we defined the Lyapunov exponent for a* 1*-dimensional map, relating it to the leading eigenvalue of an evolution operator, and promised to evaluate it. Now we are finally in position to deliver on our promise.*

The cycle averaging formula (20.26) yields an exact explict expression for the Lyapunov exponent in terms of prime cycles:

$$\lambda = \frac{1}{\langle n \rangle_\zeta} \sum{}' (-1)^{k+1} \frac{\log|\Lambda_{p_1}| + \cdots + \log|\Lambda_{p_k}|}{|\Lambda_{p_1} \cdots \Lambda_{p_k}|} \ . \tag{20.30}$$

For a repeller, the $1/|\Lambda_p|$ *weights are replaced by (22.10), the normalized measure weights* $\exp(\gamma n_p)/|\Lambda_p|$*, where* γ *is the escape rate.*

For 2-dimensional Hamiltonian flows such as our game of pinball (see example 19.3), there is only one expanding eigenvalue and (20.30) applies as written. However, in dimensions higher than one, a correct calculation of Lyapunov exponents requires a bit of sophistication.

20.5 Cycle expansions for finite alphabets

A finite transition graph like the one given in figure 14.6 (d) is a compact encoding of the transition matrix for a given subshift. It is a sparse matrix, and the associated determinant (15.20) can be written by inspection: it is the sum of all possible partitions of the graph into products of non-intersecting loops, with each loop carrying a minus sign:

$$\det(1-T) = 1 - t_0 - t_{0011} - t_{0001} - t_{00011} + t_0 t_{0011} + t_{0011} t_{0001} \tag{20.31}$$

The simplest application of this determinant is the evaluation of the topological entropy; if we set $t_p = z^{n_p}$, where n_p is the length of the p-cycle, the determinant reduces to the topological polynomial (15.21).

The determinant (20.31) is exact for the finite graph figure 14.6 (e), as well as for the associated finite-dimensional transfer operator of example 17.5. For the associated (infinite dimensional) evolution operator, it is the beginning of the cycle expansion of the corresponding dynamical zeta function:

$$\begin{aligned} 1/\zeta \ = \ & 1 - t_0 - t_{0011} - t_{0001} + t_{0001} t_{0011} \\ & -(t_{00011} - t_0 t_{0011} + \ldots \text{curvatures}) \ldots \end{aligned} \tag{20.32}$$

The cycles $\overline{0}$, $\overline{0001}$ and $\overline{0011}$ are the *fundamental* cycles introduced in (20.7); they are not shadowed by any combinations of shorter cycles. All other cycles appear together with their shadows (for example, the $t_{00011} - t_0 t_{0011}$ combination, see figure 1.12) and yield exponentially small corrections for hyperbolic systems. For cycle counting purposes, both t_{ab} and the pseudo-cycle combination $t_{a+b} = t_a t_b$ in (20.2) have the same weight $z^{n_a+n_b}$, so all curvature combinations $t_{ab} - t_a t_b$ vanish exactly, and the topological polynomial (15.27) offers a quick way of checking the fundamental part of a cycle expansion.

The splitting of cycles into the fundamental cycles and the curvature corrections depends on balancing long cycles t_{ab} against their pseudo-trajectory shadows $t_a t_b$. If the $\overline{ab}$ cycle or either of the shadows $\overline{a}$, $\overline{b}$ do not to exist, such curvature cancelation is unbalanced.

The most important lesson of the pruning of the cycle expansions is that prohibition of a finite subsequence imbalances the head of a cycle expansion and increases the number of the fundamental cycles in (20.7). Hence the pruned expansions are expected to start converging only *after* all fundamental cycles have been incorporated - in the last example, the cycles $\overline{1}$, $\overline{10}$, $\overline{10100}$, $\overline{1011100}$. Without cycle expansions, no such crisp and clear cut definition of the fundamental set of scales is available.

Because topological zeta functions reduce to polynomials for finite grammars, only a few fundamental cycles exist and long cycles can be grouped into curvature combinations. For example, the fundamental cycles in exercise 9.6 are the three 2-cycles that bounce back and forth between two disks and the two 3-cycles that visit every disk. Of all cycles, the 2-cycles have the smallest Floquet exponent, and the 3-cycles the largest. It is only after these fundamental cycles have been included that a cycle expansion is expected to start converging smoothly, i.e., only for n larger than the lengths of the fundamental cycles are the curvatures $\hat{c}_n$ (in expansion (20.7)), a measure of the deviations between long orbits and their short cycle approximations, expected to fall off rapidly with n.

20.6 Stability ordering of cycle expansions

> There is never a second chance. Most often there is not even the first chance.
>
> —John Wilkins

(C.P. Dettmann and P. Cvitanović)

We have judiciously deployed the 3-disk pinball, with its simple grammar, to motivate the periodic orbit theory. Most dynamical systems of interest, however, have infinite grammar, so at any order in z a cycle expansion may contain unmatched terms that do not fit neatly into the almost canceling curvature corrections. Similarly, for the intermittent systems that we shall discuss in sect. 24.3.4, curvature corrections are not small in general, so again the cycle expansions may converge slowly. For such systems, schemes that collect the pseudocycle terms according to some criterion other than the topology of the flow may converge faster than expansions based on the topological length.

All chaotic systems exhibit some degree of shadowing, and a good truncation criterion should do its best to respect the shadowing as much as possible. If a long cycle is shadowed by two or more shorter cycles and the flow is smooth, the periods and the Floquet exponents will be additive in sense that the period of the longer cycle is approximately the sum of the shorter cycle periods. Similarly, as

stability is multiplicative, shadowing is approximately preserved by including all terms with pseudo-cycle stability

$$\left|\Lambda_{p_1}\cdots\Lambda_{p_k}\right| \le \Lambda_{\max} \tag{20.33}$$

and ignoring any pseudo-cycles that are less stable.

Two such schemes for ordering cycle expansions that approximately respect shadowing are truncations by the pseudocycle period and the stability ordering that we shall discuss here. In these schemes, a dynamical zeta function or a spectral determinant is expanded. One keeps all terms for which the period, action or stability for a combination of cycles (pseudo-cycles) is less than a given cutoff.

Settings in which stability ordering may be preferable to ordering by topological cycle length are the cases of bad grammar, of intermittency, and of partial cycle data sets.

20.6.1 Stability ordering for bad grammars

For generic flows it is often not clear what partition of state space generates the "optimal" symbolic dynamics. Stability ordering does not require understanding dynamics in such detail: if you can find the cycles, you can use stability-ordered cycle expansions. Stability truncation is thus easier to implement for a generic dynamical system than the curvature expansions (20.7) that rely on finite subshift approximations to a given flow.

Cycles can be detected numerically by searching a long trajectory for near recurrences. The long trajectory method for detecting cycles preferentially finds the least unstable cycles, regardless of their topological length. Another practical advantage of the method (in contrast to blind Newton method searches) is that it preferentially finds cycles in a given connected ergodic component of state space, ignoring isolated cycles or other ergodic regions elsewhere in state space.

Why should stability-ordered cycle expansions of a dynamical zeta function converge better than the crude trace formula (22.9), to be discussed in sect. 22.2? The argument has essentially already been laid out in sect. 15.6: in truncations that respect shadowing, most of the pseudo-cycles appear in shadowing combinations and nearly cancel, while only the relatively small subset affected by the increasingly long pruning rules is not shadowed. The error is typically of the order of $1/\Lambda$, which is smaller by a factor e^{hT} than the trace formula (22.9) error, where h is the entropy and T is the typical cycle length for cycles of stability Λ.

20.6.2 Smoothing

 If most, but not all long cycles in a stability truncation are shadowed by shorter cycles, we say that the shadowing is partial. The breaking of exact shad-

owing cancellations deserves further comment. Any partial shadowing that may be present can be (partially) restored by smoothing the stability-ordered cycle expansions by replacing the $1/\Lambda$ weight for each term with the pseudo-cycle stability $\Lambda = \Lambda_{p_1} \cdots \Lambda_{p_k}$ by $f(\Lambda)/\Lambda$. Here, $f(\Lambda)$ decreases monotonically from $f(0) = 1$ to $f(\Lambda_{\max}) = 0$. The lack of smoothing means we have a step function.

A typical "shadowing error" induced by the cutoff is due to two pseudo-cycles of stability Λ separated by $\Delta\Lambda$; the contributions of these pseudo-cycles are of opposite sign. Ignoring possible weighting factors, the magnitude of the resulting term is of order $1/\Lambda - 1/(\Lambda + \Delta\Lambda) \approx \Delta\Lambda/\Lambda^2$. With smoothing, one obtains an extra term of the form $f'(\Lambda)\Delta\Lambda/\Lambda$, which we want to minimize. A reasonable guess might be to keep $f'(\Lambda)/\Lambda$ constant and as small as possible, so that

$$f(\Lambda) = 1 - \left(\frac{\Lambda}{\Lambda_{\max}}\right)^2$$

The results of a stability-ordered expansion (20.33) should always be tested for robustness by varying the cutoff $\Lambda_{\max}$. If this introduces significant variations, smoothing is probably necessary.

Résumé

A *cycle expansion* is a series representation of a dynamical zeta function, trace formula or a spectral determinant, with products in (19.15) expanded as sums over *pseudo-cycles*, which are products of the prime cycle weights t_p.

If a flow is hyperbolic and has the topology of the Smale horseshoe (a subshift of finite type), dynamical zeta functions are holomorphic (have only poles in the complex s plane), the spectral determinants are entire, and the spectrum of the evolution operator is discrete. The situation is considerably more reassuring than what practitioners of quantum chaos fear; there is no 'abscissa of absolute convergence' and no 'entropy barier', the exponential proliferation of cycles is no problem, spectral determinants are entire and converge everywhere, and the topology dictates the choice of cycles to be used in cycle expansion truncations.

In this case, the basic observation is that the motion in low-dimensional dynamical systems is organized around a few *fundamental* cycles, with the cycle expansion of the Euler product

$$1/\zeta = 1 - \sum_f t_f - \sum_n \hat{c}_n,$$

regrouped into dominant *fundamental* contributions t_f and decreasing *curvature* corrections $\hat{c}_n$. The fundamental cycles t_f have no shorter approximations; they are the 'building blocks' of the dynamics in the sense that all longer orbits can be

approximately pieced together from them. A typical curvature contribution to $\hat{c}_n$ is the *difference* of a long cycle $\{ab\}$ and its shadowing approximation by shorter cycles $\{a\}$ and $\{b\}$, as in figure 1.12:

$$t_{ab} - t_a t_b = t_{ab}(1 - t_a t_b / t_{ab})$$

Orbits that follow the same symbolic dynamics, such as $\{ab\}$ and a 'pseudo-cycle' $\{a\}\{b\}$, lie close to each other, have similar weights, and for increasingly long orbits the curvature corrections fall off rapidly. Indeed, for systems that satisfy the 'axiom A' requirements, such as the 3-disk billiard, curvature expansions converge very well.

Once a set of the shortest cycles has been found, and the cycle periods, stabilities, and integrated observable have been computed, the cycle averaging formulas such as (20.25) for the dynamical zeta function

$$\begin{aligned} \langle a \rangle &= \langle A \rangle_\zeta \, / \, \langle T \rangle_\zeta \\ \langle A \rangle_\zeta &= -\frac{\partial}{\partial \beta} \frac{1}{\zeta} = \sum{}' A_\pi t_\pi \,, \qquad \langle T \rangle_\zeta = \frac{\partial}{\partial s} \frac{1}{\zeta} = \sum{}' T_\pi t_\pi \end{aligned}$$

yield the expectation value of the observable $a(x)$, i.e., the long time average over the chaotic non–wandering set).

Commentary

Remark 20.1 Pseudocycle expansions. Bowen's introduction of shadowing ϵ-pseudo-orbits [1.28] was a significant contribution to Smale's theory. The expression 'pseudo-orbits' seems to have been introduced in Parry and Pollicott's 1983 paper [20.16]. Following them, M. Berry [20.9] used the expression 'pseudo-orbits' in his 1986 paper on Riemann zeta and quantum chaos. Cycle and curvature expansions of dynamical zeta functions and spectral determinants were introduced in refs. [20.10, 20.2]. Some literature [19.12] refers to pseudo-orbits as 'composite orbits', and to cycle expansions as 'Dirichlet series' (see also appendix I.5 and remark I.1).

Remark 20.2 Cumulant expansion. To statistical mechanicians, curvature expansions are very reminiscent of cumulant expansions. Indeed, (20.15) is the standard Plemelj-Smithies cumulant formula for the Fredholm determinant.A new aspect, not reminiscent of statistical mechanics, is that in cycle expansions each Q_n coefficient is expressed as a sum over exponentially many cycles.

Remark 20.3 Exponential growth of the number of cycles. Going from $N_n \approx N^n$ periodic points of length n to M_n prime cycles reduces the number of computations from N_n to $M_n \approx N^{n-1}/n$. The use of discrete symmetries (chapter 21) reduces the number

of nth level terms by another factor. While reformulating theory from trace (18.28) to cycle expansion (20.7) does not eliminate exponential growth in the number of cycles, in practice only the shortest cycles are used, and the reduction in computational labor for these cycles can be significant.

Remark 20.4 Shadowing cycle-by-cycle. A glance at the low order curvatures in table 20.1 leads to the temptation to associate curvatures to individual cycles, such as $\hat{c}_{0001} = t_{0001} - t_0 t_{001}$. Such combinations tend to be numerically small (see, for example, ref. [20.3], table 1). However, splitting $\hat{c}_n$ into individual cycle curvatures is not possible in general [20.12]; the first example of such ambiguity in the binary cycle expansion is given by the t_{100101}, t_{100110} $0 \leftrightarrow 1$ symmetric pair of 6-cycles; the counterterm $t_{001}t_{011}$ in table 20.1 is shared by these two cycles.

Remark 20.5 Escape rates. A lucid introduction to escape from repellers is given by Kadanoff and Tang [22.10]. For a review of transient chaos see refs. [22.11, 22.13]. The ζ–function formulation is given by Ruelle [22.14] and W. Parry and M. Pollicott [22.15] and discussed in ref. [22.16]. **PC** Aug 28, 2008: Altmann and Tel [22.17] give a detailed study of escape rates, with citations to more recent literature.

Remark 20.6 Stability ordering. The stability ordering was introduced by Dahlqvist and Russberg [20.13] in a study of chaotic dynamics for the $(x^2y^2)^{1/a}$ potential. The presentation here runs along the lines of Dettmann and Morriss [20.14] for the Lorentz gas, which is hyperbolic but with highly pruned symbolic dynamics, and Dettmann and Cvitanović [20.15] for a family of intermittent maps. In the applications discussed in the above papers, stability ordering yields a considerable improvement over topological length ordering. In quantum chaos applications, cycle expansion cancelations are affected by the phases of pseudo-cycles (their actions), hence *period* or *action ordering* rather than stability is frequently employed.

Remark 20.7 Desymmetrized cycle expansions. The 3-disk cycle expansions (20.35) might be useful for cross-checking purposes, but, as we shall see in chapter 21, they are not recommended for actual computations, as the factorized zeta functions yield much better convergence.

Exercises

20.1. **Cycle expansions.** Write programs that implement *binary* symbolic dynamics cycle expansions for (a) dynamical zeta functions, (b) spectral determinants. Combined with the cycles computed for a 2-branch repeller or a 3-disk system they will be useful in the problems below.

20.2. **Escape rate for a 1-dimensional repeller.** (continuation of exercise 19.1 - easy, but long) Consider again the quadratic map (19.31)

$$f(x) = Ax(1-x)$$

on the unit interval. In order to be definitive, take either $A = 9/2$ or $A = 6$. Describing the itinerary of any trajectory by the binary alphabet $\{0, 1\}$ ('0' if the iterate is in the first half of the interval and '1' if it is in the second half), we have a repeller with a complete binary symbolic dynamics.

(a) Sketch the graph of f and determine its two fixed points $\overline{0}$ and $\overline{1}$, along with their stabilities.

(b) Sketch the two branches of f^{-1}. Determine all the prime cycles up to topological length 4 using your calculator and backwards iteration of f (see sect. 13.2.1).

(c) Determine the leading zero of the zeta function (19.15) using the weights $t_p = z^{n_p}/|\Lambda_p|$, where Λ_p is the stability of the p-cycle.

(d) Show that for $A = 9/2$ the escape rate of the repeller is $0.361509\ldots$ using the spectral determinantwith the same cycle weight. If you have taken $A = 6$, show instead that the escape rate is in $0.83149298\ldots$, as shown in solution 20.2. Compare the coefficients of the spectral determinant and the zeta function cycle expansions. Which expansion converges faster?

(Per Rosenqvist)

20.3. **Escape rate for the Ulam map.** (Medium; repeat of exercise 13.1) We will try to compute the escape rate for the Ulam map (11.5)

$$f(x) = 4x(1-x),$$

using the method of cycle expansions. The answer should be zero, as nothing escapes.

(a) Compute a few of the stabilities for this map. Show that $\Lambda_0 = 4$, $\Lambda_1 = -2$, $\Lambda_{01} = -4$, $\Lambda_{001} = -8$ and $\Lambda_{011} = 8$.

(b) Show that

$$\Lambda_{\epsilon_1\ldots\epsilon_n} = \pm 2^n$$

and determine a rule for the sign.

(c) (hard) Compute the dynamical zeta function for this system

$$\zeta^{-1} = 1 - t_0 - t_1 - (t_{01} - t_0 t_1) - \cdots$$

Note that the convergence as a function of the truncation cycle length is slow. Try to fix that by treating the $\Lambda_0 = 4$ cycle separately. (continued as exercise 20.12)

20.4. **Pinball escape rate, semi-analytical.** Estimate the 3-disk pinball escape rate for $R : a = 6$ by substituting analytical cycle stabilities and periods (see exercise 13.7 and exercise 13.8) into the appropriate binary cycle expansion. Compare your result with the numerical estimate exercise 17.3.

20.5. **Pinball escape rate, from numerical cycles.** Compute the escape rate for the 3-disk pinball with $R : a = 6$ by substituting the list of numerically computed cycle stabilities of exercise 13.5 into the binary cycle expansion.

20.6. **Pinball resonances in the complex plane.** Plot the logarithm of the absolute value of the dynamical zeta function and/or the spectral determinant cycle expansion (20.5) as contour plots in the complex s plane. Do you find zeros other than the one corresponding to the complex one? Do you see evidence for a finite radius of convergence for either cycle expansion?

20.7. **Counting the 3-disk psudocycles.** (continuation of exercise 15.12) Show that the number of terms in the 3-disk pinball curvature expansion (20.34) is given by

$$\begin{aligned}\prod_p \left(1 + t_p\right) &= \frac{1 - 3z^4 - 2z^6}{1 - 3z^2 - 2z^3} \\ &= 1 + 3z^2 + 2z^3 + \frac{z^4(6 + 12z + 2z^2)}{1 - 3z^2 - 2z^3} \\ &= 1 + 3z^2 + 2z^3 + 6z^4 + 12z^5 \\ &\quad +20z^6 + 48z^7 + 84z^8 + 184z^9 + \ldots\end{aligned}$$

This means that, for example, c_6 has a total of 20 terms, in agreement with the explicit 3-disk cycle expansion (20.35).

20.8. **3–disk unfactorized zeta cycle expansions.** Check that the curvature expansion (20.2) for the 3-disk pinball, assuming no symmetries between disks, is given by

$$\begin{aligned} 1/\zeta &= (1-z^2t_{12})(1-z^2t_{13})(1-z^2t_{23}) \\ &\quad (1-z^3t_{123})(1-z^3t_{132})(1-z^4t_{1213}) \\ &\quad (1-z^4t_{1232})(1-z^4t_{1323})(1-z^5t_{12123})\cdots \\ &= 1-z^2t_{12}-z^2t_{23}-z^2t_{31}-z^3(t_{123}+t_{132}) \\ &\quad -z^4[(t_{1213}-t_{12}t_{13})+(t_{1232}-t_{12}t_{23}) \\ &\quad +(t_{1323}-t_{13}t_{23})] \\ &\quad -z^5[(t_{12123}-t_{12}t_{123})+\cdots]-\cdots \end{aligned} \tag{20.34}$$

Show that the symmetrically arranged 3-disk pinball cycle expansion of the Euler product (20.2) (see table 15.5 and figure 9.1) is given by:

$$\begin{aligned} 1/\zeta &= (1-z^2t_{12})^3(1-z^3t_{123})^2(1-z^4t_{1213})^3 \\ &\quad (1-z^5t_{12123})^6(1-z^6t_{121213})^6 \\ &\quad (1-z^6t_{121323})^3\ldots \\ &= 1-3z^2\,t_{12}-2z^3\,t_{123}-3z^4\,(t_{1213}-t_{12}^2) \\ &\quad -6z^5\,(t_{12123}-t_{12}t_{123}) \\ &\quad -z^6\,(6\,t_{121213}+3\,t_{121323}+t_{12}^3-9\,t_{12}t_{1213}-t_{123}^2) \\ &\quad -6z^7\,(t_{1212123}+t_{1212313}+t_{1213123}+t_{12}^2t_{123} \\ &\quad -3\,t_{12}t_{12123}-t_{123}t_{1213}) \\ &\quad -3z^8\,(2\,t_{12121213}+t_{12121313}+2\,t_{12121323} \\ &\quad +2\,t_{12123123}+2\,t_{12123213}+t_{12132123} \\ &\quad +3\,t_{12}^2t_{1213}+t_{12}t_{123}^2-6\,t_{12}t_{121213} \\ &\quad -3\,t_{12}t_{121323}-4\,t_{123}t_{12123}-t_{1213}^2)-\cdots \end{aligned} \tag{20.35}$$

20.9. **4–disk unfactorized dynamical zeta function cycle expansions.** For the symmetrically arranged 4-disk pinball, the symmetry group is C_{4v}, which is of order 8. The degenerate cycles can have multiplicities 2, 4 or 8 (see table 15.3). Show that:

$$\begin{aligned} 1/\zeta &= (1-z^2t_{12})^4(1-z^2t_{13})^2(1-z^3t_{123})^8 \\ &\quad (1-z^4t_{1213})^8(1-z^4t_{1214})^4(1-z^4t_{1234})^2 \\ &\quad (1-z^4t_{1243})^4(1-z^5t_{12123})^8(1-z^5t_{12124})^8 \\ &\quad (1-z^5t_{12134})^8(1-z^5t_{12143})^8 \\ &\quad (1-z^5t_{12313})^8(1-z^5t_{12413})^8\cdots . \end{aligned} \tag{20.36}$$

Show that the cycle expansion is given by

$$\begin{aligned} 1/\zeta &= 1-z^2(4\,t_{12}+2\,t_{13})-8z^3\,t_{123} \\ &\quad -z^4(8\,t_{1213}+4\,t_{1214}+2\,t_{1234}+4\,t_{1243} \\ &\quad -6\,t_{12}^2-t_{13}^2-8\,t_{12}t_{13}) \\ &\quad -8z^5(t_{12123}+t_{12124}+t_{12134}+t_{12143}+t_{12313} \\ &\quad +t_{12413}-4\,t_{12}t_{123}-2\,t_{13}t_{123}) \\ &\quad -4z^6(2\,S_8+S_4+t_{12}^3+3\,t_{12}^2\,t_{13}+t_{12}t_{13}^2 \\ &\quad -8\,t_{12}t_{1213}-4\,t_{12}t_{1214} \\ &\quad -2\,t_{12}t_{1234}-4\,t_{12}t_{1243} \\ &\quad -4\,t_{13}t_{1213}-2\,t_{13}t_{1214}-t_{13}t_{1234} \\ &\quad -2\,t_{13}t_{1243}-7\,t_{123}^2)-\cdots \end{aligned}$$

where in the coefficient of z^6 ,the abbreviations S_8 and S_4 stand for the sums over the weights of the 12 orbits with multiplicity 8 and the 5 orbits with multiplicity 4, respectively; the orbits are listed in table 15.5.

20.10. **Escape rate for the Rössler flow.** (continuation of exercise 13.10) Try to compute the escape rate for the Rössler flow (2.17) using the method of cycle expansions. The answer should be zero, as nothing escapes. Ideally you should already have computed the cycles and have an approximate grammar, but failing that you can cheat a bit and peak into exercise 13.10.

20.11. **State space volume contraction, recycled.** (continuation of exercise 4.3) The plot of instantaneous state space volume contraction as a function of time in exercise 4.3 (d) illustrates one problem of time-averaging in chaotic flows - the observable might vary wildly across each recurrence to a given Poincaré section. Evaluated on a given short cycle, the average is crisp and arbitrarily accurate. Recompute $\langle \partial \cdot v \rangle$ by means of cycle expansion, study its convergence. $1/t$ convergence of mindless time-averaging is now replaced by exponential convergence in the cycle length.

20.12. **Ulam map is conjugate to the tent map.** (continuation of exercise 20.3, repeat of exercise 6.4 and exercise 13.2; requires real smarts, unless you look it up) Explain the magically simple form of cycle stabilities of exercise 20.3 by constructing an explicit smooth conjugacy (6.1)

$$g^t(y_0) = h \circ f^t \circ h^{-1}(y_0)$$

that conjugates the Ulam map (11.5) into the tent map (11.4).

20.13. **Continuous vs. discrete mean return time.** Show that the expectation value $\langle a \rangle$ time-averaged over continuous time flow is related to the corresponding average $\langle a \rangle_{\rm dscr}$ measured in discrete time (e.g. , Poincaré section returns) by (20.29):

$$\langle a \rangle_{\rm dscr} = \langle a \rangle \langle T \rangle_\zeta / \langle n \rangle_\zeta \ . \tag{20.37}$$

(Hint: consider the form of their cycle expansions.) The mean discrete period $\langle n \rangle_\zeta$ averaged over cycles, and the mean continuous time period $\langle T \rangle_\zeta$ need to be evaluated only once, thereafter one can compute either $\langle a \rangle$ or $\langle a \rangle_{\rm dscr}$, whichever is more convenient.

References

[20.1] P. Cvitanović, *Phys. Rev. Lett.* **61**, 2729 (1988).

[20.2] R. Artuso, E. Aurell and P. Cvitanović, "Recycling of strange sets I: Cycle expansions," *Nonlinearity* **3**, 325 (1990).

[20.3] R. Artuso, E. Aurell and P. Cvitanović, "Recycling of strange sets II: Applications," *Nonlinearity* **3**, 361 (1990).

[20.4] S. Grossmann and S. Thomae, *Z. Naturforsch.* **32 a**, 1353 (1977); reprinted in ref. [20.5].

[20.5] *Universality in Chaos*, P. Cvitanović, ed., (Adam Hilger, Bristol 1989).

[20.6] F. Christiansen, P. Cvitanović and H.H. Rugh, *J. Phys* **A 23**, L713 (1990).

[20.7] J. Plemelj, "Zur Theorie der Fredholmschen Funktionalgleichung," *Monat. Math. Phys.* **15**, 93 (1909).

[20.8] F. Smithies, "The Fredholm theory of integral equations," *Duke Math.* **8**, 107 (1941).

[20.9] M.V. Berry, in *Quantum Chaos and Statistical Nuclear Physics*, ed. T.H. Seligman and H. Nishioka, *Lecture Notes in Physics* **263**, 1 (Springer, Berlin, 1986).

[20.10] P. Cvitanović, "Invariant measurements of strange sets in terms of cycles," *Phys. Rev. Lett.* **61**, 2729 (1988).

[20.11] B. Eckhardt and G. Russberg, *Phys. Rev.* **E 47**, 1578 (1993).

[20.12] E. Aurell, 'Convergence of Dynamical Zeta Functions," *J. Stat. Phys.* **58**, 967 (1990).

[20.13] P. Dahlqvist and G. Russberg, "Periodic orbit quantization of bound chaotic systems," *J. Phys.* **A 24**, 4763 (1991); P. Dahlqvist *J. Phys.* **A 27**, 763 (1994).

[20.14] C. P. Dettmann and G. P. Morriss, *Phys. Rev. Lett.* **78**, 4201 (1997).

[20.15] C. P. Dettmann and P. Cvitanović, "Cycle expansions for intermittent diffusion," *Phys. Rev. E* **56**, 6687 (1997); `arXiv:chao-dyn/9708011`.

[20.16] W. Parry and M. Pollicott, *Ann. Math.* **118**, 573 (1983).